Journal of Theoretical and Applied Information Technology
15th January 2023. Vol.101. No 1

ISSN: 1992-8645 www.jatit.org E-ISSN: 1817-3195

ZEALOUS PARTICLE SWARM OPTIMIZATION BASED RELIABLE MULTI-LAYER PERCEPTRON NEURAL NETWORKS FOR AUTISM SPECTRUM DISORDER CLASSIFICATION

B.SURESH KUMAR[1],D. JAYARAJ[2]

[1]Assistant Professor, Department of Computer and Information Science, Affiliation, Annamalai University, India
[2]Assistant Professor, Department of Computer Science Engineering, Annamalai University, India
E-mail: [1]sureshaucis@gmail.com, [2]jayarajvnr@gmail.com

ABSTRACT

Individuals with autism spectrum disorder (ASD) struggle with social interaction and learning skills throughout their lives. An early and precise diagnosis of ASD is crucial for designing an all-encompassing rehabilitation programme that enhances the individual's quality of life and facilitates their integration into their social, familial, and professional environments. However, because of its dependence on a specialist's opinion, the accuracy of ASD diagnoses is frequently compromised by the attendant lack of objectivity-related biases. As a result, several studies have focused on using deep learning and optimization to provide ASD early detection methods. This paper aims to provide a novel approach to ASD classification that uses neural networks in conjunction with optimization, namely Zealous Particle Swarm Optimization-based Reliable Multi-Layer Perceptron Neural Networks (ZPSO-RMLPNN). $ZPSO-RMLPNN$ uses different protocols and fitness scores to evaluate the fMRI more deeply to confirm the presence and absence of ASD. $ZPSO-RMLPNN$ uses threshold values to evaluate fMRI images. $ZPSO-RMLPNN$ is evaluated with the Autism Brain Imaging Data Exchange version II (ABIDE II) dataset using standard deep learning metrics. The results make an indication that $ZPSO-RMLPNN$ has superior performance than the current classifiers in terms of identifying ASD and non-ASD.

Keywords: *Autism, Classification, Optimization, Neural Network, Multi-Layer Perceptron, Particle Swarm*

1. INTRODUCTION

Image processing is a more refined illustration of the digitization and execution of operations on an image or a technique for extracting meaningful information from such a scene. The field of image processing that deals with classifying images are enormous. The classification process ensures that previously unclassified photos are placed in the appropriate groupings. In computer vision, the challenge of image categorization encompasses various fundamental data from industries, including medicine, agriculture, meteorology, and public security. The human brain may easily categorize images. But if the image is noisy, the computer will have difficulty doing this. The categorization process may be carried out in a variety of ways now. There are two classification procedures: (i) supervised classification, where an expert observes the data as it is sorted, and (ii) unsupervised classification. More data will be analyzed annually, and more information will be sorted into different categories.

Nowadays, everyone with access to a digital camera and a computer may use image processing software regularly. Low-effort methods exist for improving photos in several ways, including contrast and edge detection, intensity quantification, and application of several mathematical operations. While these methods can provide impressive results, the average user employs them carelessly, obscuring the fundamental concepts underpinning the most fundamental image-processing procedures. Though this may be comfortable with some people, it typically results in a drastically deteriorated image. It fails to deliver the outcomes that may be

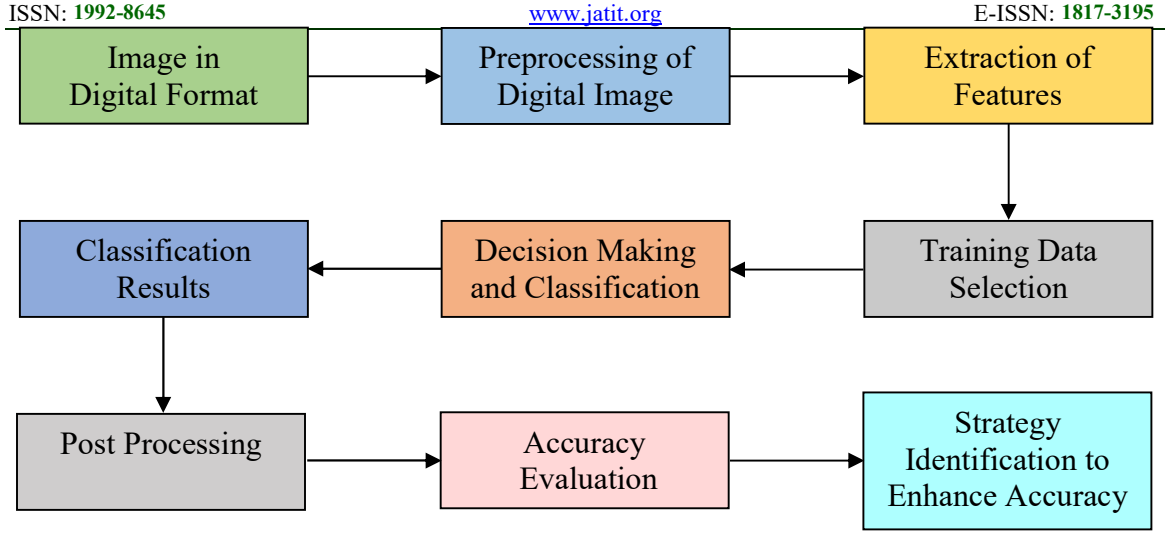

Fig 1. Image Classification Process

accomplished with familiarity with the fundamentals of an image-processing system. Figure 1 depicts the process involved in image classification.

1.1 Autism Spectrum Disorder

The social impairments and ritualistic habits that characterize Autism spectrum disorder (ASD) result from a neurological condition. Research in the field of psychiatric neuroimaging primarily seeks to locate objective biomarkers that may assist in detecting and providing treatment for persons with brain-based diseases [1]. A spectrum of phenotypes is linked with ASD, with varying impairments in social interaction, language skills, and sensory processing. Machine Learning (ML) techniques have recently been used to brain imaging data to understand better how the brain works. These algorithms can extract strong neural patterns from the brain imaging data of people with mental disorders. Machine learning is a subfield of AI that teaches computers to automatically and efficiently evaluate data to discover patterns and make judgments [2]. It is possible to use mathematical models to make predictions about the category to which a set of data points belongs using training data in supervised machine learning, which is used for classification. Classifiers trained by machine learning can model high-dimensional inputs with fewer data. As a result of their computational efficiency and applicability to small sample sizes, standard supervised machine-learning methods have been utilized to recognize abnormal motion and postural features [3]. Decision Trees, Random Forests, Support Vector Machines, K-Nearest Neighbor, Naive Bayes, Discriminant Analysis, and so on are all examples of popular algorithms. Not every method will be optimal for every dataset because of variations in feature sets, sample sizes, and data formats. Researchers typically use many supervised machine-learning algorithm variants for classification and prediction before settling on the most effective [4].

ASD encompasses various symptoms and diagnoses. Those with ASD exhibit wide variation in the severity of their symptoms, language skills, and ability in other developmental domains (such as adaptive skills and executive functioning). Some people progress slowly or reach a plateau, while others regress and lose abilities they had previously gained, and these symptoms might appear at different times for each person [5]. People on the autism spectrum may often struggle with another mental health condition. Although the exact origin of ASD is unknown, both genetics and environmental factors have been implicated. More than a hundred genes have been related to ASD, and it is believed that 10%-20% of ASD cases have genetic variations [6]. In addition, persons with a family history of autism or other developmental abnormalities have a greater incidence of autism spectrum disorder than the general population. ASD may also be influenced by exposure to certain environmental elements. Risk factors for ASD include prenatal exposures, older parents, longer intervals between pregnancies, and delivery problems. Despite discovering several environmental and genetic linkages, no one factor has been implicated in all instances of ASD. Eye-gaze performance, cognitive function, and possible pregnancy risk factors of people with ASD have all been evaluated using machine learning algorithms [7].

Additionally, machine learning classifiers were used to distinguish between usual and abnormal hand motions in persons with ASD [8]. To the best of our knowledge, however, no research has yet used machine learning methods to investigate aspects of postural control in children with ASD. Machine learning can improve ASD diagnosis by accurately identifying autistic postural control characteristics [9].

1.2 Problem Statement

ASD is difficult to treat since its genetic markers vary from patient to patient. A genetic diagnosis may be vital in deciding patient care and appropriate medicines since each individual requires a unique course of action. Identifying and understanding the causes that generate distinct varieties of ASD is crucial to create specific therapies for persons with ASD. Clinicians would benefit greatly from trustworthy and accurate technology that can easily automate the entire genetic diagnosis procedure. Early diagnosis of ASD allows for quicker intervention and improved long-term results. Another significant benefit of using a deep learning strategy for diagnosing ASD is cost savings. In 2014, the median family was estimated to spend AUD 34,900 annually [10]. In INR, it would averagely cost around Rs. 17,82,432.35.

1.3 Objective

The significant objective of this research is to propose a classification algorithm; namely, Zealous Particle Swarm Optimization Based Reliable Multi-Layer Perceptron Neural Networks, to effectively identify the presence of ASD in fMRI images, i.e., ABIDE II dataset.

1.4 Organization of the Paper

The current section of the paper has provided an overview of processes involved in digital image processing, ASD, problem statement, and objective. Section 2 provides a literature review on the subject of ASD classification. In Section 3, we propose a deep learning technique based on bio-inspiration for identifying ASD. The ABIDE II dataset is summarized in Section 4. Metrics for comparing the effectiveness of the proposed classifier to those of already-existing classifiers are detailed in Section 5. In Section 6, we analyze the obtained results. Section 7 concludes the research with future improvements.

2. LITERATURE REVIEW

"Tactile Stimulation Device" [11] is designed for the early identification of autism among infants in the proposed study. The multisensory device is presented with visual, audio, and touch data. The peripheral response data are recorded, and the stroking speed and skin force are considered. The investigation is carried out on 10-20-month-old toddlers, and responses are observed to generate the results. "Clustering Technique" [12] is applied to detect abnormal brain activity in ASD children. The centrality and network entropy measures are applied to detect the subsystem of the brain, and the functionalities are observed. The clusters are formed based on the cerebellar, and results are generated to portray the level of understanding about the tools in therapeutic diagnosis and interventions. The "Robot-mediated Imitation Skill Training Architecture" [13] technique is used in the presented study for detecting the autism level among children by operating the automated robot in diagnosis. Experiments were carried out to test the functionality and performance documentation. Results show better compatibility than traditional algorithms. "Closed-Loop Autonomous Computer System" [14] is proposed to train young toddlers affected with ASD through social skill training. The child's response is examined and monitored based on the technique's working. Toddlers were used for demonstrating, which is proven to apply to early disease diagnosis.

"Virtual Reality-based Driven System" [15] is developed a study for fusing multimodal data to enhance the driving skills of ASD-affected adolescents. The cognitive load is measured, and optimal learning skill is enhanced. Feature extraction and classification tasks are carried out, and information is fused. Results are generated to prove its convenience in increasing the driving skills of individuals. "Collaborative Virtual Environment" [16] is designed to exhibit ASD disease among children in the proposed study. Simple hand gestures of the children are monitored, and games are structured by moving the virtual objects hand-hand. The game strategies and gaze and voice-based data are taken into consideration and improve the collaboration skills of autistic children. "De-Biased Statistical Inference" [17] is proposed for validating the hypothesis of estimating the graphical models of high dimensional data of ASD. The minimization algorithm is integrated, and the sparse matrix is designed. The hypothesis is tested with statistical inference, and the False

Discovery Rate is fetched. Numerical studies generate results, and performance is measured.

"Cluster GAN Network" [18] is fine-tuned using a meta-learning structure for improving the diarization of ASD. The call-Home telephonic conversation is used for experimenting, and the proposed technique's effectiveness is investigated. X-vector is employed with the method, and accuracy is detected. "Modified Expectation-Maximization Algorithm" [19] is used for designing the framework to segregate the hand gestures in images with RGB –depth format. RGB and Depth maps are grouped, and the edges are refined using hand gestures using Bayesian Networks. Experiments are carried out, and the segregated hand gestures are adjusted based on RGB edges. Integration and testing of the framework are done by using performance metrics. "Deep Learning" [20] is proposed along with a cross-dataset structure for detecting the facial images of ASD. An objective function is introduced to control the distribution of skewed labels, and the ResNet pipeline is integrated. Experiments were conducted to test the knowledge through facial datasets and improve performance in multi-site datasets. "Automatic Facial Expression Recognition" [21] is introduced in detecting ASD, Low vision, and Alzheimer's disease based on facial expressions and emotions. 3-D videos were examined, and the lighting and head pose were considered. 2.5-dimensional face data captured with RGB-D cameras is analyzed to derive characteristics for use in an automated emotion annotation method. Classification is made based on the fetched features, and accuracy is measured.

The "Nonlinear Dimensionality Reduction" [22] method is provided to measure the neural activity of ASD based on the Blood Oxygenation-Level Dependent (BOLD) technique. Leave-One-Out-Cross-Validation (LOOCV) is used for validation, and the Locally Linear Embedding of BOLD is used for optimizing the selected feature. Both time and space complexity is decreased and prove better classification for retaining the brain structures of cohorts. "Pediatric Magnetoencephalography (MEG)" [23] is used in the prediction of ASD with abnormal communication ability. The disorder is discovered with imaging modalities, and a sensing method based on spin-exchange relaxation-free (SERF) is integrated. The infant's brain reactions are detected, and the modality substrates' progress is measured. "Mathematical Framework" [24] with Diffusion Tensor Imaging is used in the proposed study for analyzing the multiple-facial models. The novel operators are defined, and a similarity metric is stated. Comparisons of different features are made and validated with healthy patients who affect them with tuberculosis and autism. "Imitation of different postures of robot" [25] is assessed in the proposed study for ASD and TD individuals (adults, children). The learning phase is used to imitate the human posture by the robot and vice versa. Neural Network is applied in the sensory-motor architecture, and the robot is learned. Results for learning are obtained from all groups and generalized. Successful applications of bio-inspired optimization have expanded into new fields like advanced networking [26]–[34], cyber security, medical image mining, share market prediction, etc.

"Genetic-Evolutionary Random Support Vector Machine (GERSVM)" [35] is developed, whereby the cluster of SVMs selects samples and characteristics at random. Alterations are made to the genetic evolution, and the reliability of the categorization system is checked. Resting-state fMRI is used to identify aberrant brain areas and diagnose autism spectrum disorder. "Functional Connectivity Complex Network Measures (FC-CNM)" [36] uses a machine learning classification method called Recursive Cluster Elimination-based Support Vector Machine (RCE-SVM) to compare the predictive accuracy of common connection metrics with that of sophisticated network measurements taken from the ABIDE dataset. FC-CNM used RCE-SVM to evaluate the prediction efficacy of three different feature sets: (a) Functional Connectivity, (b) complex network measures, and (c) fusion of both a and b. The Cluster phase organizes the features into groups, the SVM scoring calculates each group's relevance in classification, and the RCE eliminates the groups with the lowest scores.

3. ZEALOUS PARTICLE SWARM OPTIMIZATION-BASED RELIABLE MULTI-LAYER PERCEPTRON NEURAL NETWORKS

3.1 Reliable Multi-Layer Perceptron Neural Networks ($RMLPNN$)

$RMLPNN$ is considered as a significant part of the Neural Network (NN) family. An $RMLPNN$ takes a set of inputs and turns them into a set of useful outputs by using the transformation procedure. Nodes of NN are the

ISSN: 1992-8645 www.jatit.org E-ISSN: 1817-3195

building blocks of $RMLPNN$, and its three layers (i) input-layer (IL), (ii) hidden-layer (HL), and (iii) output-layer (OL), provide a hierarchical structure. The IL is responsible for transmitting the output of the previous layer. The HL is located in the middle of the IL and the OL. Multiple HL may be present in the $RMLPNN$ network. The exact number will vary from the research problem the researcher has taken. Most research work considers only a layer. By using a transfer function, the main goal of the neurons in the HL is to change the inputs into the desired outputs. The OL is where the final results are stored. The data classes determine how many neurons are present in OL.

Each neuron present in an $RMLPNN$ is hidden, and it is linked to other neurons using 2 weights, namely, (i) connection weight (t) and (ii) bias weight. Each hidden neuron's aggregated output results from an operation of summation and activation (i.e., transference). Eqn.(1) depicts the result of the product cum summing operation performed by neuron w. Subsequently, transference functions are fully utilized to map the result of the product cum summing process.

$$sum_w^n = \prod_{w=1}^{t}\left(v_w + \sum_{s=1}^{t}(n_{sw} * st_w)\right) \quad (1)$$

wherein n_{sw} is the weight of the link between s and w neurons in the hidden layer, and v_w is the bias of w neurons present in the HL. Using Eqn.(2), this research work performs the transference process.

$$q_w = \bigwedge_{w=0}^{c} g(sum_w^n) \quad (2)$$

where q_w is the w output of the neurons, w holds the value from 1 to c, and g indicates a Sigmoid function, and the Eqn.(3) is applied to compute.

$$g(sum_w^n) = \frac{1}{1 + h^{-sum_w^n}} + \overrightarrow{v_w} \quad (3)$$

After integrating the outputs of all hidden nodes, Q_w is computed by the summing and transference methods which are depicted in Eqn.(4) and Eqn.(5):

$$g(sum_w^n) = \sum_{s=1}^{c} n_{sw} * q_w + \overrightarrow{v_w} \quad (4)$$

The bias w to neuron w is represented as n_{sw}, while the link weight of HL between s and w neuron is indicated as v_w.

$$Q_w = g(sum_w^n) \quad (5)$$

where w holds the value between 1 to a, and the value of g is derived from Eqn.(3)

3.2 Zealous Particle Swarm Optimization

An innovative swarm intelligence and global optimization algorithm, Particle Swarm Optimization (PSO) algorithm takes cues from particles' social iterative behavior in the natural world. The $ZPSO$ algorithm is developed based on particles' foraging, alertness, and flying behaviors. Five protocols utilized to describe the algorithm's underlying concept are:

Protocol 1: Each particle must be in either the "watch" or "forage" position.

Protocol 2: While foraging, each particle remembers and maintains track of its own and the group's most successful strategies for finding food. This information will change where it goes and how it looks for food.

Protocol 3: Each particle in the alert condition makes a concerted effort to travel toward the center of the flock, believing that the particles in the center have more energy reserves. Predators are less likely to attack the particles in the middle.

Protocol 4: Migrating particles constantly swing back and forth between productive and subsistence activities. According to this optimization-based classification algorithm, the particles with the biggest reserves are the providers, while the ones with the lowest are the parasites. But other particles are supposed to be either leaders or followers at random.

Protocol 5: The particles that identify most foods take the lead in the quest for food, while the scavengers follow one randomly.

The $ZPSO$ algorithm's key components are modeled based on these assumptions. The

optimization begins by seeding the Y-dimensional search space with T number of particles at random. Each particle in the swarm uses its intelligent knowledge and the collective wisdom of the flock when foraging, as outlined in $Protocol\ 2$. Eqn.(6) provides a mathematical representation of $Protocol\ 2$, if $s\ \omega\ [1, \ldots . T], w\ \omega [1, \ldots , Y]$, and $rand_d$ are random numbers that are selected from the range $[0, 1]$ which are normally distributed, then $p_{s,w}^{f}$ will act as the value of component w related to s number of generations in f. The accelerated coefficients for intelligence and social interaction are the 2 significant constant positive values, namely U and E. Experience on a small scale $M_{s,w}$ and a large scale j_s are both shown in Eqn.(6).

$$p_{s,w}^{f+1} = \prod p_{s,w}^{f} + \left(m_{s,w} - p_{s,w}^{f}\right) \times \sum_{d=1}^{s} (U \times rand_d) + \left(j_w - p_{s,w}^{f}\right) \times \sum_{d=1}^{w} (E \times rand_d) \quad (6)$$

If a random number generated is more than M, this foraging behavior will be triggered. This is just a straightforward implementation of $Protocol\ 1$ in action. Eqn.(7)-Eqn.(9) derived from $Protocol\ 3$ are used in $ZBSA$'s for modeling the particles' flight toward the middle of the swarm.

$$p_{s,w}^{f+1} = \prod p_{s,w}^{f} + D1\left(mean_w - p_{s,w}^{f}\right) \times rand_d + D2\left(m_{a,w} - p_{s,w}^{f}\right) \times E \times rand_v \quad (7)$$

$$D1 = \prod_{s=1}^{w} \left(d1 \times exp\left(\frac{-mFS_s}{sumFS + \sigma} \times T \right) \right) \quad (8)$$

$$D2 = \prod d2 \times e \times xp\left(\sum_{a,s=0}^{w} \left(\frac{mFS_s - mFS_a}{|mFS_a - mFS_s| + \sigma} \right) \times \left(\frac{T \times mFS_a}{sumFS + \sigma} \right) \right) \quad (9)$$

The Fittest Score (FS) of particle s is mFS_s, where the constants of proportionality numbers $d1$ cum $d2$ fall in the range $[0, 2]$ and its sum. The mean fitness of the flock is represented by the sum of FS, where σ depicts a tiny constant used to prevent division by zero and $mean_w$ indicates a number present in wth element of the swarm in the current location.

To compensate for environmental factors, particles use the swarm's mean efficiency as they move closer to its center. $Protocol\ 4$ depicts particles that have recently finished flying, and Eqn.(10) and Eqn.(11) mathematically express the same.

$$p_{s,w}^{f+1} = \prod p_{s,w}^{f} + \sum \left(randt + p_{s,w}^{f} \right) \quad (10)$$

$$p_{s,w}^{f+1} = \prod p_{s,w}^{f} + \sum_{w=1}^{s} \left(p_{a,w}^{f} - p_{s,w}^{f} \right) \times GZ \times rand_d \quad (11)$$

where $a\ \omega\ [1, \ldots , T]$ and $a \neq s$, $GZ\omega[0,2]$ and $randt$ is a random integer generated from a Gaussian distribution with a mean value of 0 and a variance value of 1.

3.3 Fusion of ZPSO and RMLPNN

This research work has developed a $ZPSO$ optimizer to determine the best possible outline for the underlying network (weights and biases). $ZPSO$ employs a structure of $RMLPNN$ network, whereby the amount of neurons is determined by the Eqn.(12) rather than some arbitrary threshold value because there exists no threshold condition for selecting the number of hidden nodes.

$$c = \sum_{y=0}^{s} (2 \times y) + 1 \quad (12)$$

where y indicates the total amount of data characteristics, and c is the total number of neurons. Eqn.(13) is utilized to derive the sum of all weights and biases.

$$t = \sum_{c=1}^{y} \left((y * c) + (2 * c) \right) + 1 \quad (13)$$

As part of the $ZPSO$ optimizer's $RMLPNN$ network integration, weights and biases are represented by "particles" that are individuals in the optimization part. The vector containing the particle's data consists of t double-precision floating-point integers. $ZPSO$ optimizer may be used to train RMLPNN by combining $ZPSO$ operators with the $RMLPNN$ architecture. This

research work breaks this entire strategy into five different phases, which are:

Phase 1: Random Particle Construction
The proposed technique begins with the specification of the $RMLPNN$ structure, including the overall amount of biases and weights (t) and the number of neurons (c), Next, a distribution of $RMLPNN$ network representing T particles is constructed randomly.

Phase 2: Fitness Score (FS) Calculation
FS of each particle is evaluated by applying a fitness function to the training data. The MSE defined in Eqn.(14), was employed as an FS.

$$MSE = \frac{1}{a}\sum_{s=1}^{a}(q_s - \hat{q}_s)^2 \quad (14)$$

The actual output of the snd training sample is q_s, the anticipated output of the sth training sample is $\hat{q}_s$, and the overall number of training samples is a.

Phase 3: Updation
Before training $RMLPNN$, the best personal and overall FS for every particle is updated. Afterward, the state of each particle is used to alter the vector associated with that particle. To further increase the variety of the flock, the particles will be separated into two categories. Once that is done, the overall FS and its associated solution will be refreshed.

Phase 4: Termination
The iterations are repeated till they reach their maximum number.

To ensure that the resulting $RMLPNN$ can be utilized as a predictive model, the MSE is calculated using the testing samples, with the best FS. The $ZPSO$ optimizer considers the $RMLPNN$ networks discovered to generate a new set of $RMLPNN$ networks. This strategy uses the maximum number of iterations to calculate MSEs and improve the $RMLPNN$s until the end condition is met. It is worth noting that the suggested $ZPSO$-based trainer averages the MSE across all $RMLPNN$ networks for performing the classification on ABIDE-II dataset training samples. Since there are t possible random $RMLPNN$ networks, f maximum possible iterations, and y possible training samples, the computational cost is $K(tfy)$.

4. ABOUT THE DATASET

The success and value of ABIDE I's setup for aggregating functional MRI (fMRI) data from many sites were proven. The intricacy of the connectome, the great variability of ASD, and the first results from the ABIDE I data analysis all point to the necessity of much bigger and better-characterized samples, however. Therefore, ABIDE II was formed with funding from the National Institute of Mental Health (R21MH107045) to further discover work on the brain connectome in ASD. The phenotypic characterization of ABIDE II's datasets, especially those measuring core ASD and accompanying symptoms, has increased by over a thousand since the project began. In addition, two sets of information comprise longitudinal samples from 38 individuals over two different periods with intervals of one to four years. To this point, ABIDE II has 19 sites involved, including 10 charter institutions and 7 new members, who contributed 1114 datasets containing data on 521 people affected with ASD and 593 controls in the range of 5-64 years. In June 2016, this information was made publicly available to researchers. No personally identifiable information is included in any of the datasets, as required by HIPAA and the standards used by the 1000 Functional Connectomes Project/INDI. Figure 2 provides the sample images. The fMRI images hold the pixel values of 256×256.

5. PERFORMANCE METRICS

The current research utilizes the below-mentioned standard cum benchmark performance metrics to evaluate ZPSO-RMLPNN against GERSVM and FC-CNM.

- **Classification Accuracy ($Cl - Acc$):** The accuracy of a classification system is measured by how many right predictions are made relative to overall samples.
- **F-Measure ($F - Msr$):** It is a statistic used to evaluate the reliability of

classification. It is calculated as the harmonic mean (i.e., weighted mean) of the classification's recall and precision.

- **Fowlkes-Mallows Index (FMI):** It represents the geometric mean of recall and precision results.
- **Matthews Correlation Coefficient (MCC):** It denotes the true and predicted values correlation coefficient.

The metrics mentioned above make use of four variables, namely (i) True-Positive ($Tr - Pos$), (ii) False-Positive ($Fl - Pos$), (iii) True-Negative ($Tr - Neg$), and (iv) False-Negative ($Fl - Neg$).

6. RESULTS AND DISCUSSION

6.1 ASD detection by ZPSO-RMLPNN

Figure 3 highlights the autistic brain regions that are identified by the proposed classifier $ZPSO - RMLPNN$ while evaluating in MATLAB 2021b.

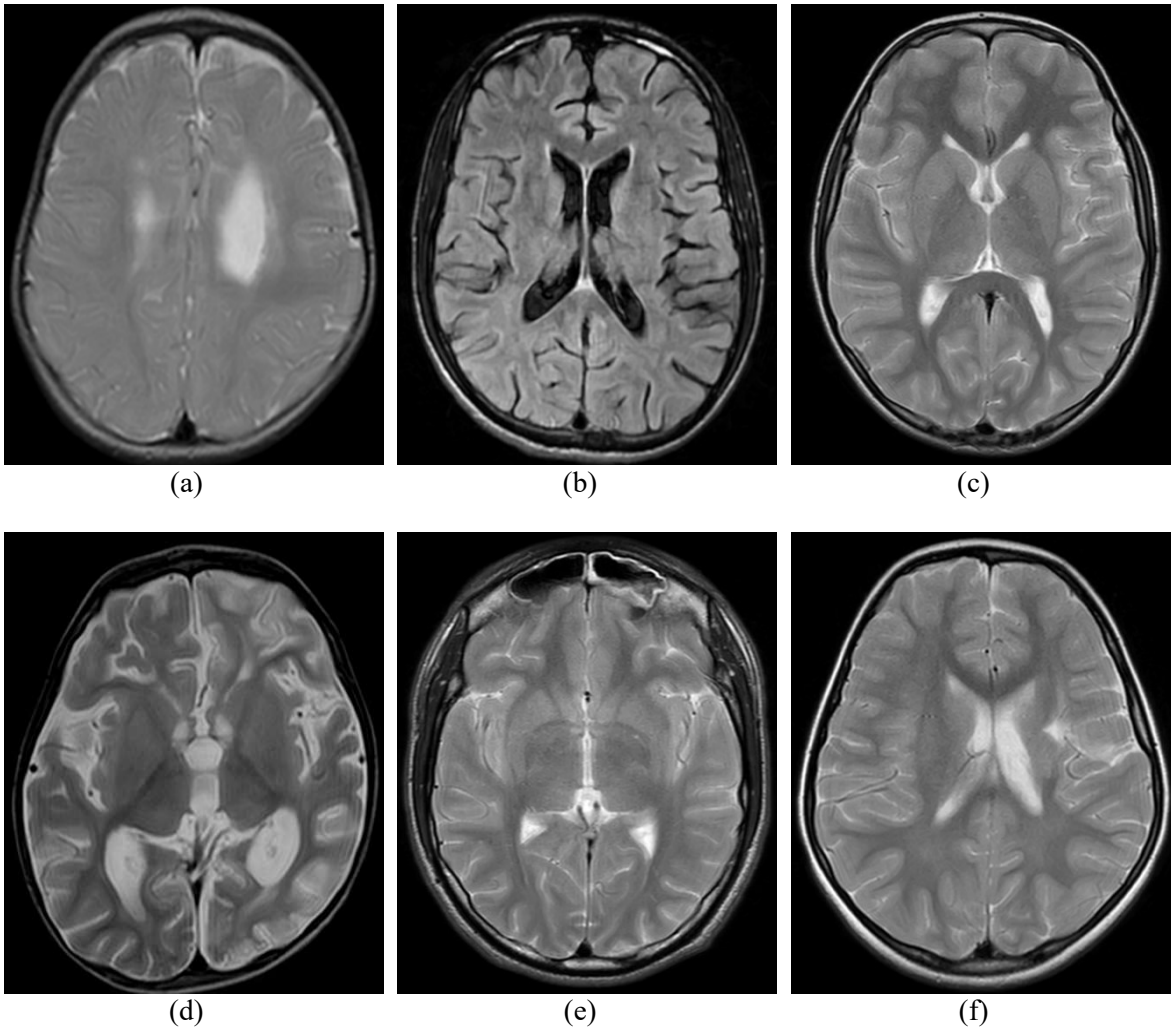

(a) (b) (c)

(d) (e) (f)

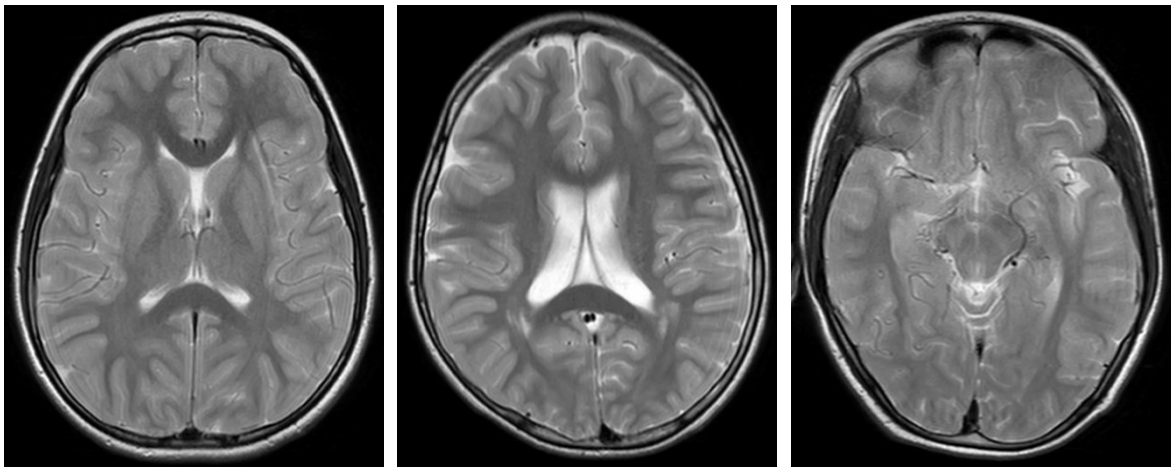

(g) (h) (i)

Fig 2 Autistic fMRI Brain Images

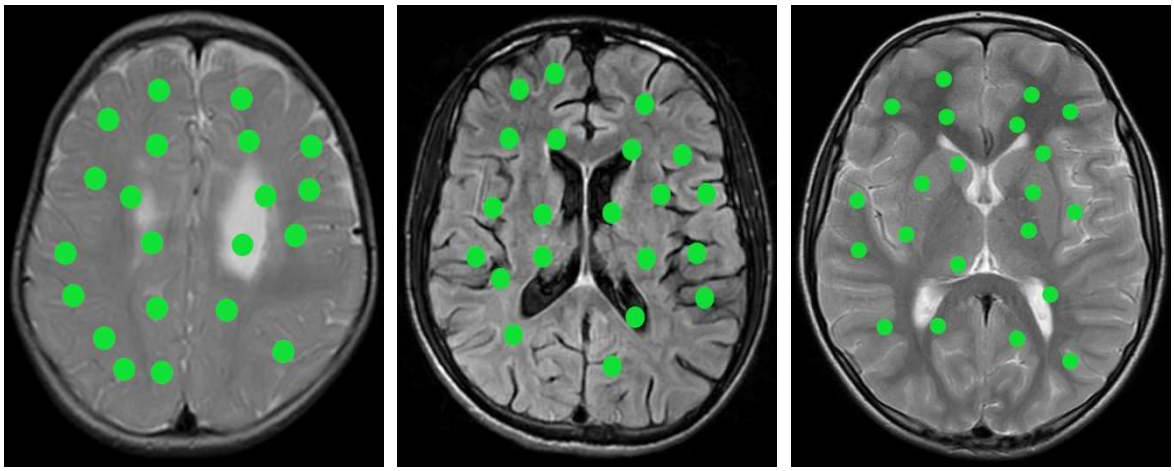

(a) (b) (c)

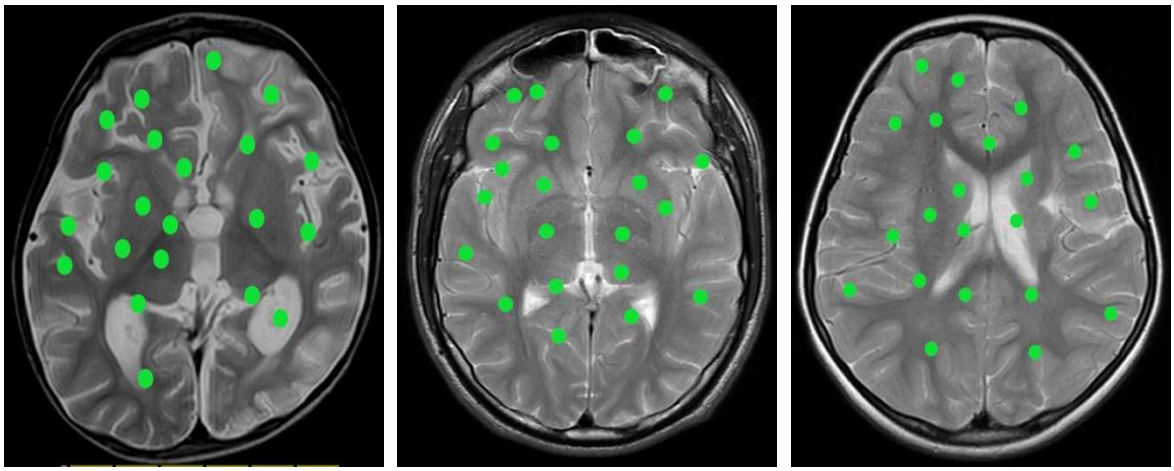

(d) (e) (f)

Journal of Theoretical and Applied Information Technology
15th January 2023. Vol.101. No 1

ISSN: 1992-8645 www.jatit.org E-ISSN: 1817-3195

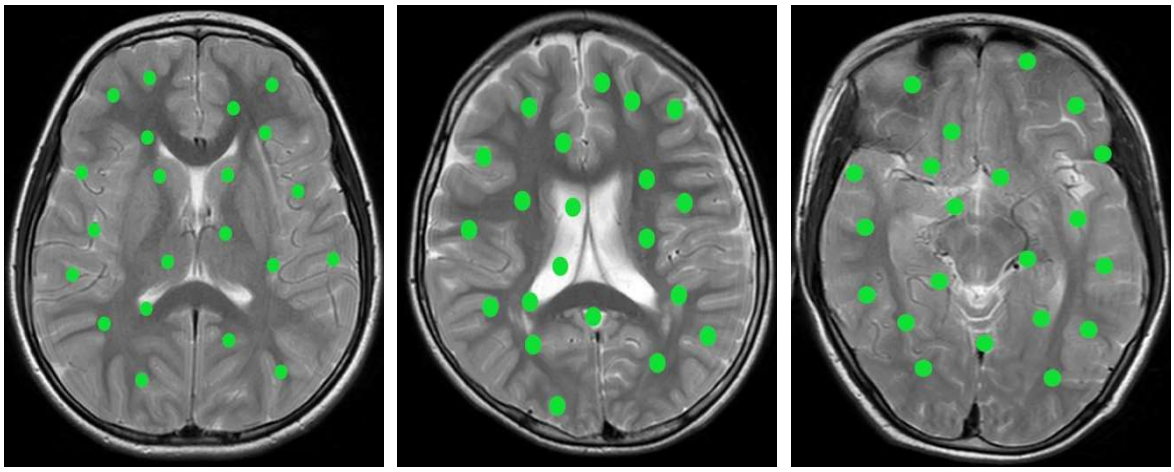

(g) (h) (i)

Fig 3 Autistic Brain Regions detected by $ZPSO - RMLPNN$

6.2 Positivity Analysis

Figure 4 analyzes the positive results (i.e., $Tr - Pos$and $Fl - Pos$) obtained during the evaluation of classifiers. The X-axis is plotted with $Tr - Pos$and $Fl - Pos$, which are variables. Y-axis is plotted with results measured in percentage. By offering higher $Tr - Pos$ and lower $Fl - Pos$, $ZPSO - RMLPNN$ has surpassed the state-of-the-art classifiers, as shown in Figure 4. Optimization in $ZPSO - RMLPNN$ plays a significant role in identifying exact ASD and non-ASD from $fMRI$ images. The state-of-the-art classifier does not perform any optimization toward identifying ASD and non-ASD more accurately. The values of $Tr - Pos$and $Fl - Pos$ results that were determined during the evaluation of classifiers are included in Table 1.

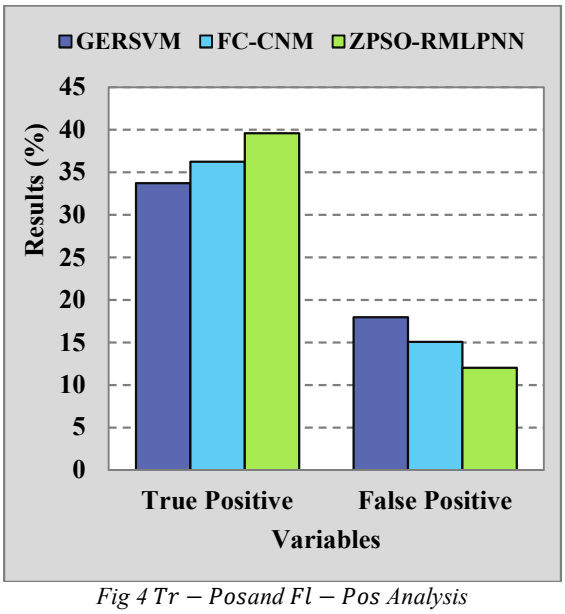

Fig 4 $Tr - Pos$and $Fl - Pos$ Analysis

Table 1 $Tr - Pos$and $Fl - Pos$ Result Values

Algorithm	$Tr - Pos$	$Fl - Pos$
GERSVM	33.752	17.953
FC-CNM	36.266	15.081
ZBSO-MLPNN	39.587	12.029

6.3 Negativity Analysis

Evaluation of negative results (i.e., $Tr - Neg$ and $Fl - Neg$) are carried out in Figure 5. The $X - axis$ displays $Tr - Neg$ and $Fl - Neg$ as independent variables. The $Y - axis$ displays percentages of $Tr - Neg$ and $Fl - Neg$results. Figure 5 demonstrates that $ZPSO - RMLPNN$ is superior to the other available classifiers since it offers higher $Tr - Neg$ with lower $Fl - Neg$. $ZPSO - RMLPNN$ classifies ASD and non-ASD optimistically. Five different protocols used by $ZPSO - RMLPNN$ lead to better $Tr - Neg$ and lower $Fl - Neg$ than the state-of-the-art classifiers, where no protocols are used to identify ASD and non-ASD accurately. Table 2 holds the values of $Tr - Neg$ and $Fl - Neg$results that were established during the assessment of classifiers.

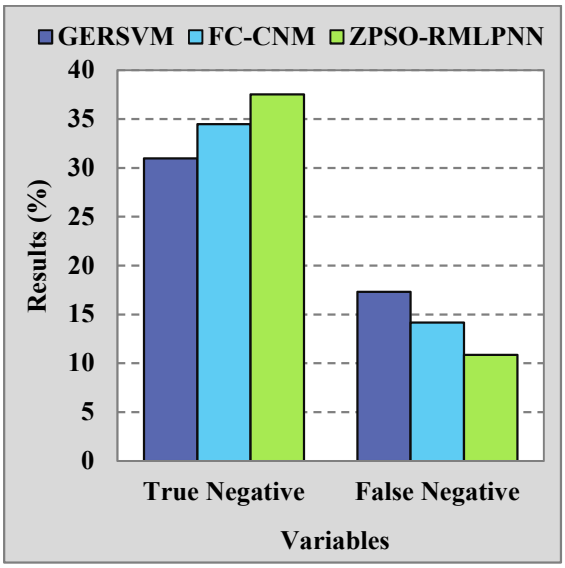

Fig 5 $Tr-Negand\ Fl-Neg$ Analysis

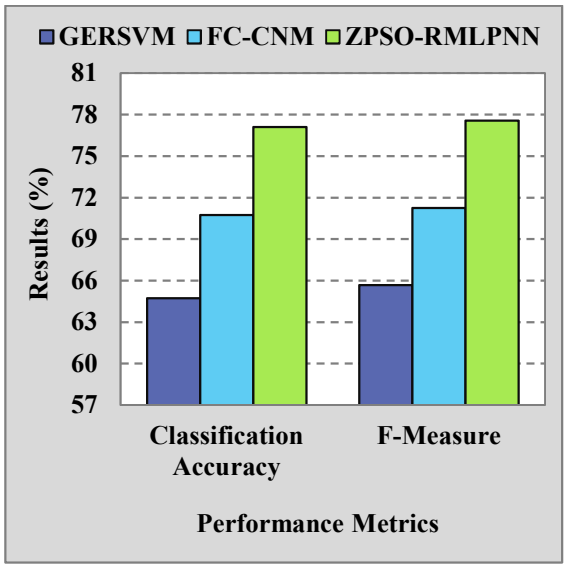

Fig 6 $Cl-Acc$ and $F-Msr$ Analysis

Table 2 $Tr-Negand\ Fl-Neg$ Result Values

Algorithm	$Tr-Neg$	$Fl-Neg$
GERSVM	30.969	17.325
FC-CNM	34.470	14.183
ZBSO-MLPNN	37.522	10.862

Table 3 $Cl-Acc$ and $F-Msr$ Result Values

Algorithm	$Cl-Acc$	$F-Msr$
GERSVM	64.722	65.677
FC-CNM	70.736	71.252
ZBSO-MLPNN	77.110	77.573

6.4 $Cl-Acc$ and $F-Msr$ Analysis

$Cl-Acc$ and $F-Msr$ results of the proposed classifier and existing classifiers are analyzed in Figure 6. $Cl-Acc$ and $F-Msr$ are marked in $X-axis$, where the $Y-axis$ represents the percentage of obtained results. Fitness score (FS) plays a vital role in achieving the better $Cl-Acc$ and $F-Msr$. $ZPSO-RMLPNN$ evaluates every fMRI based on the fitness score. If the FS is high, then $ZPSO-RMLPNN$ confirms the presence of ASD, and if the FS is low, then $ZPSO-RMLPNN$ confirms the absence of ASD. Existing classifiers does not profoundly evaluate the fMRI using any FS and which leads them to face low $Cl-Acc$ and poor $F-Msr$. The values of $Cl-Acc$ and $F-Msr$results that were determined during the evaluation of classifiers are included in Table 3.

6.5 FMI and MCC Analysis

A comparison of the proposed and current classifiers for FMI and MCC outcomes is shown in Figure 7. FMI and MCC measurements are shown on the $X-axis$, while the outcomes are shown on the $Y-axis$. The sigmoid function present in $RMLPNN$ and the updation strategy of $ZPSO$, works together to achieve the better FMI and MCC. The better FMI and MCC indicate how many levels the ASD and non-ASD are classified accurately. State-of-the-art classifiers do not use applying any function to detect ASD and non-ASD, which leads to achieving better FMI and MCC. Table 4 displays the results obtained for both proposed and existing classifiers for the FMI and MCC measures.

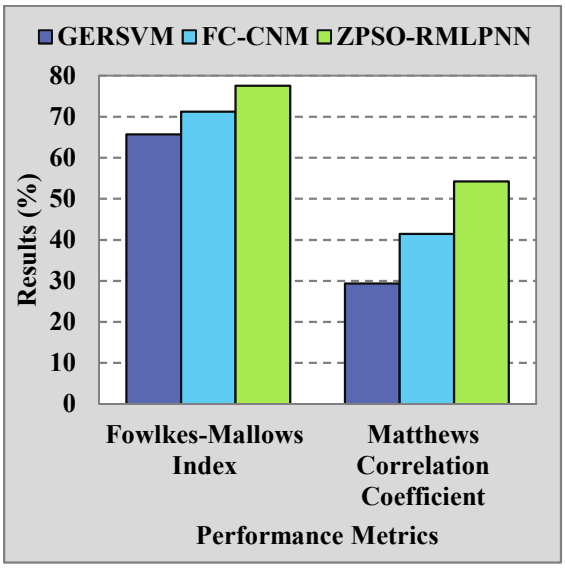

Fig 7 FMI and MCC Analysis

Table 4 FMI and MCC Result Values

Algorithm	*FMI*	*MCC*
GERSVM	65.678	29.394
FC-CNM	71.255	41.465
ZBSO-MLPNN	77.578	54.221

7. CONCLUSION

Autism spectrum disorder (ASD) is complex since there is a large range of the presence of co-morbid behavioral and medical problems, and it is not understood how these diseases affect the capacity to detect ASD. Predictive models based on optimization are seeing a widespread application for locating patterns that can serve as biomarkers for various neuropathological diseases. This paper proposed Zealous Particle Swarm Optimization Based Reliable Multi-Layer Perceptron Neural Networks (ZPSO-RMLPNN) to classify ASD with better reliability. Different strategies are performed in the optimization and classification stages of $ZPSO-RMLPNN$. The fitness function plays a great role in achieving better results, where the score of the fitness function is used to confirm the presence and absence of ASD. $ZPSO-RMLPNN$ is evaluated with ABIDE-II dataset using significant deep learning metrics. $ZPSO-RMLPNN$ has achieved 77.11% of classification accuracy, where the existing classifiers have achieved 67.729% of classification accuracy only. Results indicate that $ZPSO-RMLPNN$ can be applied in healthcare to assist experts in confirming the presence of ASD that leads to saving of cost spent in diagnosing ASD. The future scope of this research work can focus on utilizing different bio-inspired optimization strategies to classify ASD more accurately.

REFERENCES:

[1] R. Filipovych, S. M. Resnick, and C. Davatzikos, "JointMMCC: Joint maximum-margin classification and clustering of imaging data," *IEEE Trans. Med. Imaging*, vol. 31, no. 5, pp. 1124–1140, 2012, doi: 10.1109/TMI.2012.2186977.

[2] F. Ke, S. Choi, Y. H. Kang, K.-A. Cheon, and S. W. Lee, "Exploring the Structural and Strategic Bases of Autism Spectrum Disorders With Deep Learning," *IEEE Access*, vol. 8, pp. 153341–153352, 2020, doi: 10.1109/ACCESS.2020.3016734.

[3] D. Fabiano, S. Canavan, H. Agazzi, S. Hinduja, and D. Goldgof, "Gaze-based classification of autism spectrum disorder," *Pattern Recognit. Lett.*, vol. 135, pp. 204–212, Jul. 2020, doi: 10.1016/j.patrec.2020.04.028.

[4] L. Chetcuti *et al.*, "Temperament in individuals with Autism Spectrum Disorder: A systematic review," *Clin. Psychol. Rev.*, vol. 85, p. 101984, 2021, doi: https://doi.org/10.1016/j.cpr.2021.101984.

[5] F. Thabtah, "Machine learning in autistic spectrum disorder behavioral research: A review and ways forward," *Informatics for Health and Social Care*, vol. 44, no. 3. Taylor and Francis Ltd, pp. 278–297, Jul. 03, 2019. doi: 10.1080/17538157.2017.1399132.

[6] B. D. Needham *et al.*, "Plasma and Fecal Metabolite Profiles in Autism Spectrum Disorder," *Biol. Psychiatry*, vol. 89, no. 5, pp. 451–462, 2021, doi: https://doi.org/10.1016/j.biopsych.2020.09.025.

[7] D. E. Lidstone, R. Rochowiak, C. Pacheco, B. Tunçgenç, R. Vidal, and S. H. Mostofsky, "Automated and scalable Computerized Assessment of Motor Imitation (CAMI) in children with Autism Spectrum Disorder using a single 2D camera: A pilot study," *Res.*

Autism Spectr. Disord., vol. 87, p. 101840, 2021, doi: https://doi.org/10.1016/j.rasd.2021.101840.

[8] G. Tan, K. Xu, J. Liu, and H. Liu, "A Trend on Autism Spectrum Disorder Research: Eye Tracking-EEG Correlative Analytics," *IEEE Trans. Cogn. Dev. Syst.*, vol. 14, no. 3, pp. 1232–1244, 2022, doi: 10.1109/TCDS.2021.3102646.

[9] M. M. Hassan and H. M. O. Mokhtar, "AutismOnt: An Ontology-Driven Decision Support For Autism Diagnosis and Treatment," *Egypt. Informatics J.*, vol. 23, no. 1, pp. 95–103, 2022, doi: https://doi.org/10.1016/j.eij.2021.07.002.

[10] C. Horlin, M. Falkmer, R. Parsons, M. A. Albrecht, and T. Falkmer, "The Cost of Autism Spectrum Disorders," *PLoS One*, vol. 9, no. 9, p. 106552, Sep. 2014, doi: 10.1371/JOURNAL.PONE.0106552.

[11] D. Bian *et al.*, "A Novel Multisensory Stimulation and Data Capture System (MADCAP) for Investigating Sensory Trajectories in Infancy," *IEEE Trans. Neural Syst. Rehabil. Eng.*, vol. 26, no. 8, pp. 1526–1534, 2018, doi: 10.1109/TNSRE.2018.2854672.

[12] J. R. Sato, M. C. Vidal, S. de S. Santos, K. B. Massirer, and A. Fujita, "Complex Network Measures in Autism Spectrum Disorders," *IEEE/ACM Trans. Comput. Biol. Bioinforma.*, vol. 15, no. 2, pp. 581–587, 2018, doi: 10.1109/TCBB.2015.2476787.

[13] Z. Zheng, E. M. Young, A. R. Swanson, A. S. Weitlauf, Z. E. Warren, and N. Sarkar, "Robot-Mediated Imitation Skill Training for Children With Autism," *IEEE Trans. Neural Syst. Rehabil. Eng.*, vol. 24, no. 6, pp. 682–691, 2016, doi: 10.1109/TNSRE.2015.2475724.

[14] Z. Zheng *et al.*, "Design of an Autonomous Social Orienting Training System (ASOTS) for Young Children With Autism," *IEEE Trans. Neural Syst. Rehabil. Eng.*, vol. 25, no. 6, pp. 668–678, 2017, doi: 10.1109/TNSRE.2016.2598727.

[15] L. Zhang *et al.*, "Cognitive Load Measurement in a Virtual Reality-Based Driving System for Autism Intervention," *IEEE Trans. Affect. Comput.*, vol. 8, no. 2, pp. 176–189, 2017, doi: 10.1109/TAFFC.2016.2582490.

[16] H. Zhao, A. R. Swanson, A. S. Weitlauf, Z. E. Warren, and N. Sarkar, "Hand-in-Hand: A Communication-Enhancement Collaborative Virtual Reality System for Promoting Social Interaction in Children With Autism Spectrum Disorders," *IEEE Trans. Human-Machine Syst.*, vol. 48, no. 2, pp. 136–148, 2018, doi: 10.1109/THMS.2018.2791562.

[17] X. Lyu, W. W. Sun, Z. Wang, H. Liu, J. Yang, and G. Cheng, "Tensor Graphical Model: Non-Convex Optimization and Statistical Inference," *IEEE Trans. Pattern Anal. Mach. Intell.*, vol. 42, no. 8, pp. 2024–2037, 2020, doi: 10.1109/TPAMI.2019.2907679.

[18] M. Pal *et al.*, "Meta-Learning With Latent Space Clustering in Generative Adversarial Network for Speaker Diarization," *IEEE/ACM Trans. Audio, Speech, Lang. Process.*, vol. 29, pp. 1204–1219, 2021, doi: 10.1109/TASLP.2021.3061885.

[19] Z. Ju, X. Ji, J. Li, and H. Liu, "An Integrative Framework of Human Hand Gesture Segmentation for Human–Robot Interaction," *IEEE Syst. J.*, vol. 11, no. 3, pp. 1326–1336, 2017, doi: 10.1109/JSYST.2015.2468231.

[20] B. Han, W.-H. Yun, J.-H. Yoo, and W. H. Kim, "Toward Unbiased Facial Expression Recognition in the Wild via Cross-Dataset Adaptation," *IEEE Access*, vol. 8, pp. 159172–159181, 2020, doi: 10.1109/ACCESS.2020.3018738.

[21] X. Zhao, J. Zou, H. Li, E. Dellandréa, I. A. Kakadiaris, and L. Chen, "Automatic 2.5-D Facial Landmarking and Emotion Annotation for Social Interaction Assistance," *IEEE Trans. Cybern.*, vol. 46, no. 9, pp. 2042–2055, 2016, doi: 10.1109/TCYB.2015.2461131.

[22] G. Sidhu, "Locally Linear Embedding and fMRI Feature Selection in Psychiatric Classification," *IEEE J. Transl. Eng. Heal. Med.*, vol. 7, 2019, doi: 10.1109/JTEHM.2019.2936348.

[23] A. Liang *et al.*, "Whole-Head Magnetoencephalogram and Its Application in Developmental Communication Disorders Research: A Review," *IEEE Access*, vol. 9, pp. 42515–42532, 2021, doi: 10.1109/ACCESS.2021.3063054.

[24] M. Taquet *et al.*, "A Mathematical Framework for the Registration and Analysis of Multi-Fascicle Models for Population Studies of the Brain Microstructure," *IEEE Trans. Med. Imaging*, vol. 33, no. 2, pp. 504–517, 2014, doi: 10.1109/TMI.2013.2289381.

[25] S. Boucenna, S. Anzalone, E. Tilmont, D. Cohen, and M. Chetouani, "Learning of Social Signatures Through Imitation Game Between a Robot and a Human Partner," *IEEE Trans. Auton. Ment. Dev.*, vol. 6, no. 3, pp. 213–225, 2014, doi: 10.1109/TAMD.2014.2319861.

[26] J. Ramkumar, "Bee inspired secured protocol for routing in cognitive radio ad hoc networks," *Indian J. Sci. Technol.*, vol. 13, no. 30, pp. 2159–2169, 2020, doi: 10.17485/ijst/v13i30.1152.

[27] J. Ramkumar and R. Vadivel, "Improved frog leap inspired protocol (IFLIP) – for routing in cognitive radio ad hoc networks (CRAHN)," *World J. Eng.*, vol. 15, no. 2, pp. 306–311, 2018, doi: 10.1108/WJE-08-2017-0260.

[28] J. Ramkumar and R. Vadivel, "Multi-Adaptive Routing Protocol for Internet of Things based Ad-hoc Networks," *Wirel. Pers. Commun.*, vol. 120, no. 2, pp. 887–909, Apr. 2021, doi: 10.1007/s11277-021-08495-z.

[29] R. Jaganathan and R. Vadivel, "Intelligent Fish Swarm Inspired Protocol (IFSIP) for Dynamic Ideal Routing in Cognitive Radio Ad-Hoc Networks," *Int. J. Comput. Digit. Syst.*, vol. 10, no. 1, pp. 1063–1074, 2021, doi: 10.12785/ijcds/100196.

[30] R. Jaganathan and V. Ramasamy, "Performance modeling of bio-inspired routing protocols in Cognitive Radio Ad Hoc Network to reduce end-to-end delay," *Int. J. Intell. Eng. Syst.*, vol. 12, no. 1, pp. 221–231, 2019, doi: 10.22266/IJIES2019.0228.22.

[31] J. Ramkumar and R. Vadivel, "CSIP—cuckoo search inspired protocol for routing in cognitive radio ad hoc networks," in *Advances in Intelligent Systems and Computing*, 2017, vol. 556, pp. 145–153. doi: 10.1007/978-981-10-3874-7_14.

[32] J. Ramkumar, C. Kumuthini, B. Narasimhan, and S. Boopalan, "Energy Consumption Minimization in Cognitive Radio Mobile Ad-Hoc Networks using Enriched Ad-hoc On-demand Distance Vector Protocol," *2022 Int. Conf. Adv. Comput. Technol. Appl. ICACTA 2022*, pp. 1–6, Mar. 2022, doi: 10.1109/ICACTA54488.2022.9752899.

[33] J. Ramkumar and R. Vadivel, "Whale optimization routing protocol for minimizing energy consumption in cognitive radio wireless sensor network," *Int. J. Comput. Networks Appl.*, vol. 8, no. 4, pp. 455–464, 2021, doi: 10.22247/ijcna/2021/209711.

[34] J. Ramkumar and R. Vadivel, "Meticulous Elephant Herding Optimization based Protocol for Detecting Intrusions in Cognitive Radio Ad Hoc Networks," *Int. J. Emerg. Trends Eng. Res.*, vol. 8, no. 8, pp. 4548–4554, 2020, doi: 10.30534/ijeter/2020/82882020.

[35] X. Bi *et al.*, "The Genetic-Evolutionary Random Support Vector Machine Cluster Analysis in Autism Spectrum Disorder," *IEEE Access*, vol. 7, pp. 30527–30535, 2019, doi: 10.1109/ACCESS.2019.2902889.

[36] N. Chaitra, P. A. Vijaya, and G. Deshpande, "Diagnostic prediction of autism spectrum disorder using complex network measures in a machine learning framework," *Biomed. Signal Process. Control*, vol. 62, p. 102099, 2020, doi: https://doi.org/10.1016/j.bspc.2020.102099.